Asian Journal of Chemistry; Vol. 34, No. 3 (2022), 557-561

ASIAN JOURNAL OF CHEMISTRY

https://doi.org/10.14233/ajchem.2022.23514

Metallophilicity *versus* π-π Interactions: Argentophilicity in Porphyrin Dimer

PRAGATI[1], AKHILESH KUMAR[2,*], AKHIL K. SINGH[3], ARVIND KUMAR PANDEY[4] and SANTOSH KUMAR SRIVASTAVA[1]

[1]Department of Chemistry, C.M.P. Degree College, Pragyagraj-211002, India
[2]Department of Chemistry, P.B.P.G. College, Prataphgarh-230002, India
[3]Institute for Inorganic Chemistry, Karlsruhe Institute of Technology, 76131 Karlsruhe, Germany
[4]Department of Chemistry, University of Allahabad, Pragyagraj-211002, India

*Corresponding author: E-mail: aks.modanwal@gmail.com

Received: 3 September 2021; *Accepted*: 26 October 2021; *Published online*: 14 February 2022; AJC-20685

The interaction between two unsupported Ag(III)porphyrins, which exist as a metalloporphyrin dimer has been studied. The UV-visible spectrum shows only slight change in Soret band position indicative of Ag(III) formation. Optimized structure of the complexes has clearly revealed that only metal-centered oxidation results in short Ag-N (porphyrin) distance with large distortion in the porphyrin macrocycle. The dispersion effect brings two rings more closer to form an unprecedented Ag(III)···Ag(III) interaction and cancel out the π-π repulsion. The interaction energy was found to be 55.34 Kcal/mol and was further supported by electron localization function, AIM analysis. The Ag(III) dimer also gives pink emission at low temperature. This type of interaction can be exploited to design several light responsive materials and molecular semiconductors.

Keywords: Metallophilic interaction, Porphyrin dimer, QTAIM analysis, Electronic structure.

INTRODUCTION

The study of interactions between closed-shell are becoming interesting area of research in recent decades due to its use in designing monumental molecular devices [1-8]. The term "metallophilicity" was suggested for the first time in 1994 by Pyykko and coworkers [6]. Although these attractive interactions of closed shell atom are clearly counter-intuitive because two positive charges should repel each other in nature. However the strength of such attractive interactions are more than classical non-covalent interactions such as π-π stalking, ion dipole, dipole-dipole interaction and has been nearly close to the energy of hydrogen bonding. These interactions are adequate enough to grant amazing structural and physical properties such as luminescence, magnetism, polychromism and one-dimensional electrical conductivity, *etc*. [1-8]. Although molecular compounds of gold based metallophilic interactions are well known in the literature however, analogous but probably weaker silver-silver interactions have been less studied. Chemistry of silver can set excellent opportunities over gold chemistry by the virtue of greater versatility in coordination numbers and geometries of the former [9-14]. The efforts to evaluate the structure and energy characteristics of argentophilic interactions are dominated by Ag(I) complexes however, the chemistry for silver (III) ions is unexplored because of high oxidizing power of Ag(II) and Ag(III) [13,14]. Furthermore, heavier d^8 transition-metal ions in square planar complexes, having large crystal field splitting are also believed to have a closed shell and therefore expected to be formed similar metallophilic interactions [6-8]. There are various metal-metal bonded porphyrin derivatives reported but all are with open shell. In present work, the effects of possible interactions between two Ag(III) porphyrins which exist as a dimer are studied.

EXPERIMENTAL

Free base octaethylporphyrine (OEP), other reagents and solvents were purchased from commercial sources and purified by standard procedures before use.

Preparation of AgOEP: A 50 mL round bottom flask was charged with a CH_2Cl_2 solution (30 mL) of OEP (50 mg, 0.09 mmol). A solution of silver acetate (30 mg, 0.18 mmol) in 5 mL of methanol/acetonitrile (1:1) was added to the flask and the mixture was refluxed for 0.5 h in an atmospheric air.

The reaction mixture was filtered through celite to remove excess metal salt and the resulting solution was evaporated to complete dryness under vacuum. The solid compound was subjected to column chromatography on silica gel. The first fraction eluted with 50% hexane/dichloromethane was collected and dried under vacuum to obtain a crimson red solid of AgOEP. The ultrapure crystalline solid, was obtained by recrystallization from dry CH_2Cl_2 solution of complex, layered carefully with *n*-hexane and kept in air for slow diffusion. On standing for 5-6 days, the product was formed as a red solid, collected and dried under vacuum [15]. Yield 40 mg (64%); UV-vis (CH_2Cl_2) [λ_{max}, nm (ε, $M^{-1}\,cm^{-1}$)]: 409 nm (1.9×10^5), 525 (0.3×10^5), 560 (0.8×10^5).

Preparation of $[AgOEP{\cdot}(PF_6)]_2$: A 50 mL round bottom flask was charged with a CH_2Cl_2 solution of AgOEP (50 mg, 0.076 mmol) and subjected to the addition of $AgPF_6$ (24 mg, 0.095 mmol) and the mixture was stirred at room temperature for 10 min. The resulting solution was then evaporated to dryness. Yield: 45 mg (74%). UV-vis (CH_2Cl_2) [λ_{max}, nm (ε, $M^{-1}\,cm^{-1}$)]: 404 nm (0.9×10^5), 515 (0.1×10^5), 550 (0.2×10^5).

Computational details: Ultraviolet-visible spectra were measured on a Perkin-Elmer UV/Vis spectrometer. The photoluminescence measurements were done with a Horiba Jobin Yvon Fluorolog-322 spectrometer at room temperature. The detector was Hamamatsu R9910 photomultiplier for the emission spectral range of about 300-830 nm. The coordinates of OEP^+ for geometry optimizations were obtained from direct drawing on gauss view software. The counter anions have not been included in calculation. Complex OEP^+ has the molecular formula $C_{74}H_{94}N_8Ag_2$. The Gaussian 09, revision B.01, package [16] used for all structure optimizations. The geometry optimizations have been done without any constraints and frequency calculations were also performed to ensure that optimized geometries don't have any imaginary frequencies [17].

Geometry optimizations have been carried out using the unrestricted dispersion corrected density functional method B97D [17]. The basis set was SDD [18] for the silver atom and 6-31G** for C, N and H atoms. Polarized continuum (PCM) model was used for dichloromethane solvent correction in all the calculations. Geometry optimization was also performed on B3LYP [19-21] hybrid functional, which does not account dispersion effects to put light on the role of dispersion into the optimized complexes. The topographical analysis of B97D optimized geometry of $AgOEP^+$ was performed by the software DAMQT. The wave functions generated with the Gaussian 09 program were further used for the QTAIM and NBO analysis by the Multiwfn [22]. Molecular orbitals and the corresponding diagrams were analyzed and sketched with the Chemcraft software [23].

RESULTS AND DISCUSSION

The ultraviolet-visible spectrum of AgOEP was recorded in CH_2Cl_2 which displays a distinct Soret and Q bands position at 409 nm, 526 and 560 nm, respectively. However, slight blue shifts was observed in comparison to the parent compound in the oxidized complex (Fig. 1); low energy broad bands are completely missing due to the formation of Ag(III) porphyrin in solution (*vide infra*). Complex $[AgOEP{\cdot}(PF_6)]_2$ gives pink emission at low temperature (77 K). The complex features a intense emission at 550 nm (Figs. 2-3). The energy difference between HOMO and LUMO of monomer and dimer has been compared and reported in Fig. 4. It has been found that the energy required for a transition from HOMO to LUMO decreases upon dimer formation, which could be reason for intense emission properties of dimer.

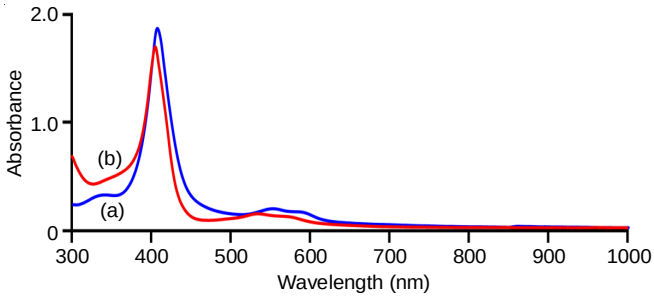

Fig. 1. UV-visible spectra (in dichloromethane at 295 K) of AgOEP (a) and $[AgOEP{\cdot}(PF_6)]_2$ (b)

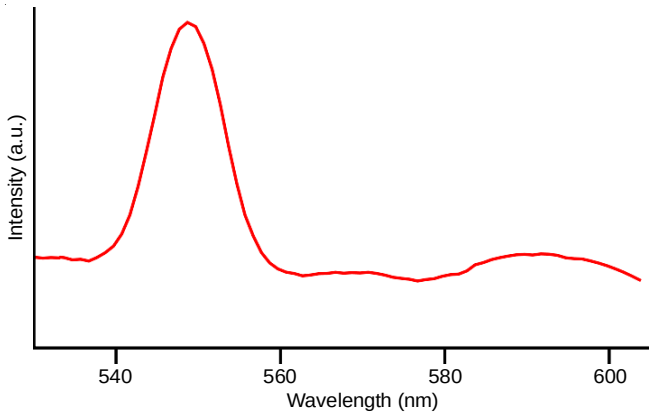

Fig. 2. (A) Normalized emission spectra of solid sample of $(AgOEP{\cdot}PF_6)_2$ at 77 K, excitation wavelength 404 nm

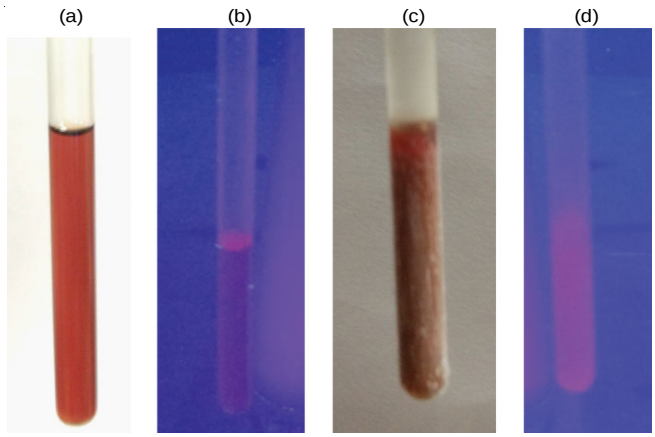

Fig. 3. Photographic image of $[AgOEP{\cdot}(PF_6)_2]$ dimer in dichloromethane at 295 K, (a) under normal light, (b) under UV light (365 nm) and at 77 K, (c) under normal light, (d) under UV light (365 nm)

Computational studies: Computational studies were done using DFT at the UB97D/SDD/6-31G** level, basis set combination, to gain more insight into the electronic structure. The geometries of $AgOEP^+$ (without counter anions) were

optimized and the calculations virtually produce the evidence of metallophilic interaction. The oxidation of silver(II) centre causes the porphyrin ring to be more distorted due to shorter Ag-N_{por} distance along with the drastic reductions of the Ag(III)···Ag(III) separation, slip angle and lateral slip between two porphyrin rings.

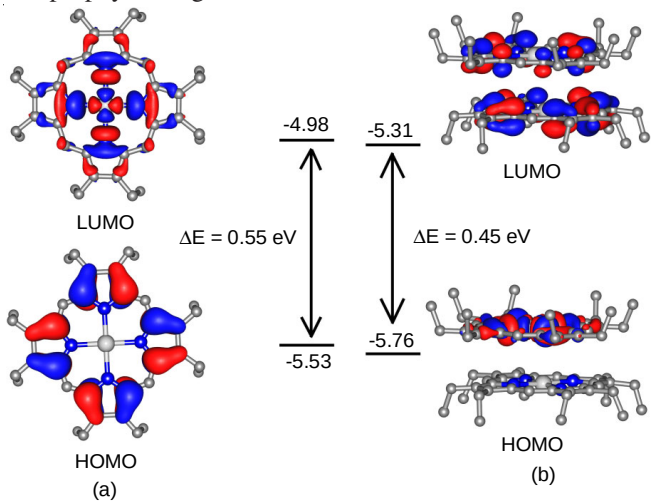

Fig. 4. Energy diagrams and selected Kohn-Sham orbitals (top view) of UB97D/SDD/LANL2DZ optimized geometry of (A) (A) $AgOEP^+$ (B) $(AgOEP^+)_2$

To investigate the role of dispersion into the optimized complexes, geometry optimization was also done using B3LYP hybrid functional, which does not involve dispersion effects. Although calculations show similar Ag-N_{por} distances as observed with UB97D, there are indeed large separation between two rings as reflected in the MPS, slip angle, lateral slip and Ag···Ag distances in $AgOEP^+$ (Fig. 5). However, inclusion of the dispersion correction by B97D causes both the rings to come closer in $AgOEP^+$ facilitating the Ag(III)···Ag(III) interaction.

For more accurate measurement of the extent of such Ag(III)···Ag(III) interaction, AIM (atoms in molecules) analysis was performed. The software DAMQT 2.1.0 was utilized for the topographical analysis of B97D/LANL2DZ/SDD optimized geometry of $AgOEP^+$. Upon single point calculations employing B97D/LANL2DZ/SDD level of theory, the electron density at the bond critical point for the Ag(III)···Ag(III) is found to be 0.011 a.u. (Fig. 6). Wiberg indices are also calculated and the bond order for Ag(III)···Ag(III) was found to be 0.008 which also supports such interaction.

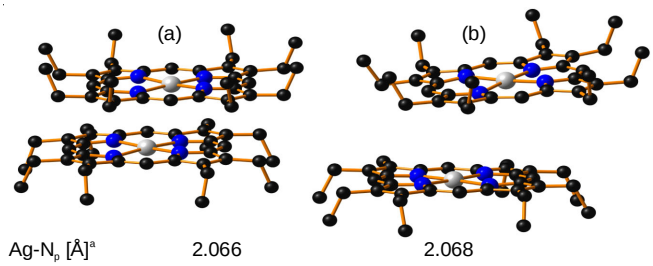

Ag-N_p [Å][a]	2.066	2.068
MPS [Å][b]	3.533	4.425
Slip angle [°][c]	25.84	38.57
Lateral shift [Å][d]	1.54	3.529
Ag···Ag [Å][e]	3.517	5.658

Fig. 5. Optimized geometries of $AgOEP^+$ at (a) UB97D/SDD/LANL2DZ, (b) UB3LYP/SDD/LANL2DZ (H-atoms have been omitted for clarity. [(a) average value, (b) average distance between the two intramolecular least-squares planes of the $C_{20}N_4$ pophyrinato core. (c) slip angle: average angle (θ) between the vector joining two macrocyclic centers and the unit vectors normal to the two macrocyclic $C_{20}N_4$ porphyrinato cores. (d) lateral shift: [sin(θ) × (Ct···Ct)]. (e) non-bonding distance]

Furthermore, the topological analysis of the electron density within the framework of Bader's theory (QTAIM method) was also carried out [24-26]. To explore the Ag···Ag interactions in silver porphyrin dimers. In the analysis, we have found bond paths (BPs) and bond critical points (BCPs) between the two Ag atoms in the atomic basins of electron density gradient contour lines map and its Laplacian distribution $\nabla^2\rho(r)$, bond critical points (3, -1), bond paths, selected zero-flux surfaces and electron localization function (ELF) map for the Ag···Ag interactions are shown in Fig. 7. The presence of a unique bond path with a bond critical point connecting two atoms is usually invoked as one criterion of interacting atoms. Besides, the

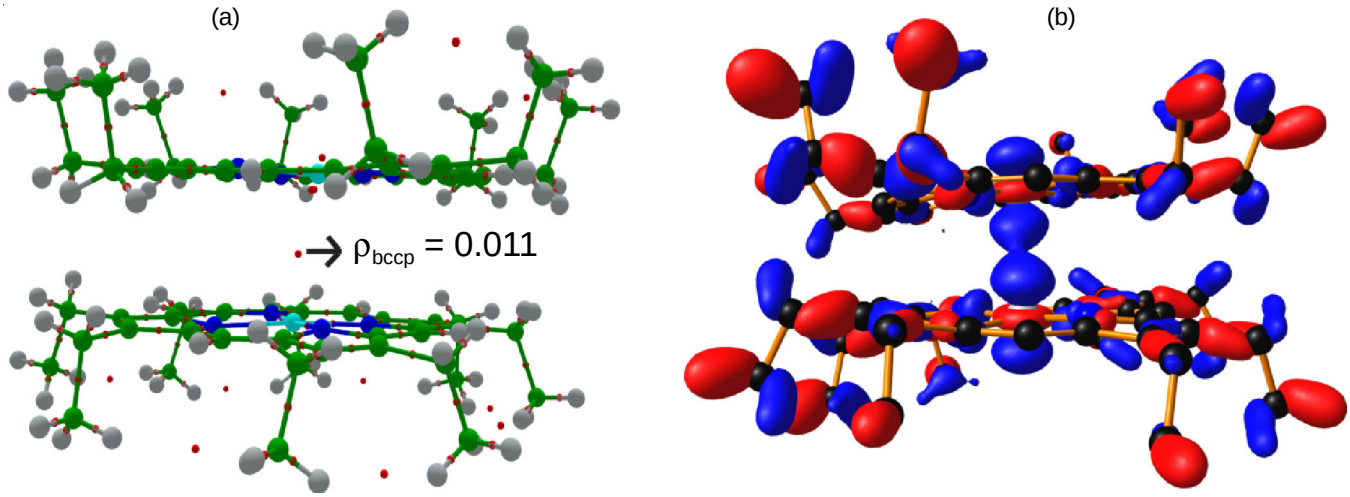

Fig. 6. (a) DAMQT 2.1.0 picture of $AgOEP^+$ showing bond critical point between two Ag(III)···Ag(III) atoms (B) orbital showing Ag···Ag interaction in $AgOEP^+$

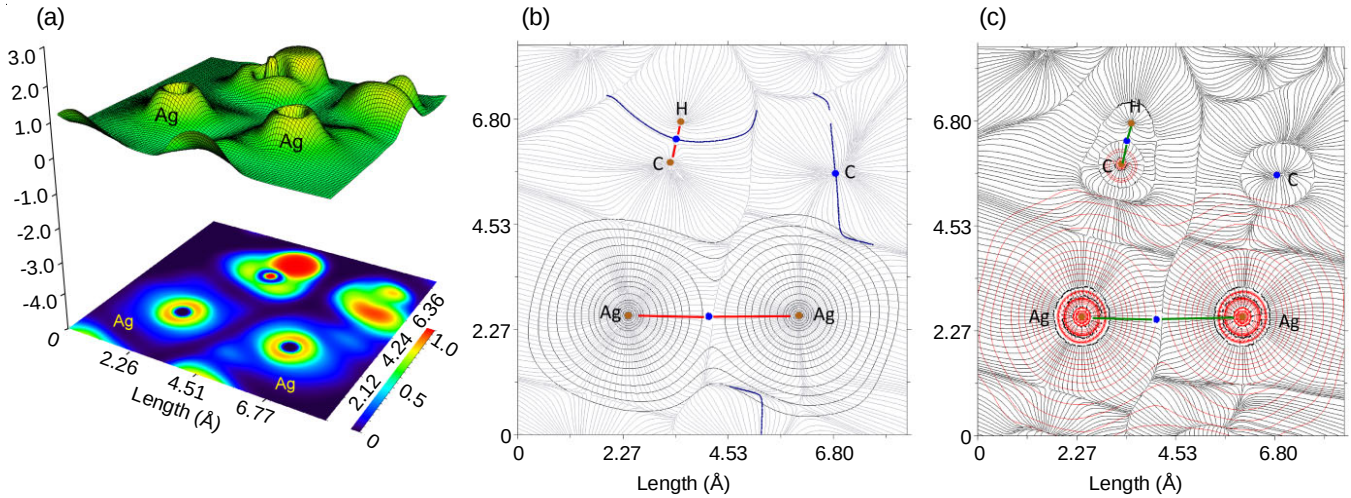

Fig. 7. QTAIM analysis of Ag···Ag interaction in $AgOEP^+$: (a) shaded surface maps of electron localization function (ELF). (b) contour line plots of the electron density ρ, (c) contour line plots of the Laplacian distribution of electron density $\nabla^2\rho(r)$, the solid (red) and dashed (blue) lines corresponds to positive and negative values of $\nabla^2\rho(r)$ respectively and (c) shaded surface maps of electron localization function (ELF). Bond paths are shown as green lines, selected zero-flux surfaces or interbasin paths as blue lines, bond critical points, BCPs, (3, -1) are shown in blue. Values of the electron density ρ and Laplacian distribution $\nabla^2\rho(r)$ at the BCBs present in between the Ag atoms are given in atomic unit (a.u)

topological properties of the electron density and its Laplacian distribution at the bond critical points have been related to the nature of the interaction between atoms.

There are two factors which govern the Ag-Ag contacts and should be responsible for the face-to-face arrangements of the complex. (i) Ag(III)-Ag(III) interaction and (ii) π-π interactions. Actually, two porphyrin rings of the dimmers should be slipped rather than ideally eclipsed one which is assigned as a geometric requirement of face-to-face π-π interaction proposed by Scheidt *et al*. [27]. In present case, two porphyrin rings are on the top of each other, which suggest that the Ag-Ag interaction is compensating the repulsion caused by two rings, mostly on top of each other in $AgOEP^+$. The interaction energy can be calculated by 2 × energy of monomer-energy of dimer and it was found to be 55.34 Kcal/mol.

Conclusion

For an attractive π-π interaction the aromatic rings should be slipped. Present investigation clearly demonstrates that metallophilic attractive interactions do play an essential role in bringing two porphyrin in $AgOEP^+$ more cofacial as evident by the short Ag(III)···Ag(III) distance. The observations are further supported by the QTAIM Analysis, ELF studies, *etc.* The Ag(III)···Ag(III) interaction further reflected reflected in pink colour emission at low temperature.

ACKNOWLEDGEMENTS

Pragati, Dr. A. Kumar, Dr. A.K. Singh and Dr. S.K. Srivastava thank C.M.P. Degree college, University of Allahabad for providing facilities.

CONFLICT OF INTEREST

The authors declare that there is no conflict of interests regarding the publication of this article.

REFERENCES

1. H. Schmidbaur and A. Schier, *Angew. Chem. Int. Ed.*, **54**, 746 (2015); https://doi.org/10.1002/anie.201405936
2. A. Cebollada, A. Vellé, M. Iglesias, L.B. Fullmer, S. Goberna-Ferrón, M. Nyman and P.J. Sanz-Miguel, *Angew. Chem. Int. Ed.*, **54**, 12762 (2015); https://doi.org/10.1002/anie.201505736
3. H. Schmidbaur and A. Schier, *Chem. Soc. Rev.*, **41**, 370 (2012); https://doi.org/10.1039/C1CS15182G
4. S. Sculfort and P. Braunstein, *Chem. Soc. Rev.*, **40**, 2741 (2011); https://doi.org/10.1039/c0cs00102c
5. A.L. Balch, *Angew. Chem. Int. Ed.*, **48**, 2641 (2009); https://doi.org/10.1002/anie.200805602
6. P. Pyykkö, *Chem. Soc. Rev.*, **37**, 1967 (2008); https://doi.org/10.1039/b708613j
7. M.J. Katz, K. Sakai and D.B. Leznoff, *Chem. Soc. Rev.*, **37**, 1884 (2008); https://doi.org/10.1039/b709061g
8. A.C. Tsipis, *Coord. Chem. Rev.*, **345**, 229 (2017). https://doi.org/10.1016/j.ccr.2016.08.005
9. J. Zheng, Y.-D. Yu, F.-F. Liu, B.-Y. Liu, G. Wei and X.-C. Huang, *Chem. Commun.*, **50**, 9000 (2014); https://doi.org/10.1039/C4CC01523A
10. J. Jin, W. Wang, Y. Liu, H. Hou and Y. Fan, *Chem. Commun.*, **47**, 7461 (2011); https://doi.org/10.1039/c1cc12142a
11. M. Kriechbaum, J. Hölbling, H.-G. Stammler, M. List, R.J.F. Berger and U. Monkowius, *Organometallics*, **32**, 2876 (2013); https://doi.org/10.1021/om300932r
12. L. Ray, M.M. Shaikh and P. Ghosh, *Inorg. Chem.*, **47**, 230 (2008); https://doi.org/10.1021/ic701830m
13. D. Daphnomili, C. Raptopoulou, A. Terzis, J.-H. Agondanou, S. Be'nazeth and A.G. Coutsolelos, *Inorg. Chem.*, **43**, 4363 (2004); https://doi.org/10.1021/ic035155x
14. J. Poulin, C. Stern, R. Guilard and P.D. Harvey, *Photochem. Photobiol.*, **82**, 171 (2006); https://doi.org/10.1562/2005-06-16-RA-577
15. T.E. Clement, D.J. Nurco and K.M. Smith, *Inorg. Chem.*, **37**, 1150 (1998); https://doi.org/10.1021/ic970774p
16. M.J. Frisch, G.W. Trucks, H.B. Schlegel, G.E. Scuseria M.A. Robb, J.R. Cheeseman, G. Scalmani, V. Barone, B. Mennucci, G.A. Petersson, H. Nakatsuji, M. Caricato, X. Li, H.P. Hratchian, A.F. Izmaylov, J. Bloino, G. Zheng, J.L. Sonnenberg, M. Hada, M. Ehara, K. Toyota, R.

Fukuda, J. Hasegawa, M. Ishida, T. Nakajima, Y. Honda, O. Kitao, H. Nakai, Vreven, J.A. Jr. T. Montgomery, J.E. Peralta, F. Ogliaro, M. Bearpark, J.J. Heyd, E. Brothers, K.N. Kudin, V.N. Staroverov, T. Keith, R. Kobayashi, J. Normand, K. Raghavachari, A. Rendell, J.C. Burant, S.S. Iyengar, J. Tomasi, M. Cossi, N. Rega, J.M. Millam, M. Klene, J.E. Knox, J.B. Cross, V. Bakken, C. Adamo, J. Jaramillo, R. Gomperts, R.E. Stratmann, O. Yazyev, A.J. Austin, R. Cammi, C. Pomelli, J. W. Ochterski, R.L. Martin, K. Morokuma, V.G. Zakrzewski, G.A. Voth, P. Salvador, J.J. Dannenberg, S. Dapprich, A.D. Daniels, Ö. Farkas, J.B. Foresman, J.V. Ortiz, J. Cioslowski and D.J. Fox, Gaussian 09, revision B.01. Gaussian, Inc.: Wallingford, CT (2010).

17. S. Grimme, *J. Comput. Chem.*, **27**, 1787 (2006); https://doi.org/10.1002/jcc.20495
18. D. Andrae, U. Häußermann, M. Dolg, H. Stoll and H. Preuß, *Theor. Chim. Acta*, **77**, 123 (1990); https://doi.org/10.1007/BF01114537
19. A.D. Becke, *J. Chem. Phys.*, **98**, 5648 (1993); https://doi.org/10.1063/1.464913
20. C. Lee, W. Yang and R.G. Parr, *Phys. Rev. B Condens. Matter*, **37**, 785 (1988); https://doi.org/10.1103/PhysRevB.37.785
21. P.J. Stephens, F.J. Devlin, C.F. Chabalowski and M. Frisch, *J. Phys. Chem.*, **98**, 11623 (1994); https://doi.org/10.1021/j100096a001
22. R. López, J.F. Rico, G. Ramírez, I. Ema, D. Zorrilla, A. Kumar, S.D. Yeole and S.R. Gadre, *Comput. Phys. Commun.*, **214**, 207 (2017); https://doi.org/10.1016/j.cpc.2017.01.012
23. T. Lu and F. Chen, *J. Comput. Chem.*, **33**, 580 (2012); https://doi.org/10.1002/jcc.22885
24. http://www.chemcraftprog.com
25. R.F.W. Bader, Atoms in Molecules: A Quantum Theory, Oxford University Press: New York (1990).
26. R.F.W. Bader, *Chem. Rev.*, **91**, 893 (1991); https://doi.org/10.1021/cr00005a013
27. W. Jentzen, J.A. Shelnutt and W.R. Scheidt, *Inorg. Chem.*, **55**, 6294 (2016); https://doi.org/10.1021/acs.inorgchem.6b00956